

Experimental analysis of the dynamic noise behavior of a two-stage cylindrical gearbox

Christian Brecher¹ · Marius Schroers¹  · Christoph Löpenhaus¹

Received: 28 June 2017 / Accepted: 27 October 2017 / Published online: 9 November 2017
© German Academic Society for Production Engineering (WGP) 2017

Abstract There are several objectives in the design phase of gears: Besides a sufficient load capacity and a high efficiency of the gearbox, the acoustic behavior has to be taken into account. For a single-stage gearbox, several research projects have been carried out regarding the improvement of the noise behavior. Because of the mutual interactions between the gear meshes at a multi-stage gearbox, the knowledge at single-stage gearboxes cannot be transferred without restrictions. In this report, experimental investigations are carried out on a two-stage test gearbox. The experimental tests are analyzed by means of the stiffness of the intermediate shaft and the number of teeth of the two gear stages. The noise generation process will be investigated by the measured signals along the machine acoustic noise generation process. First, the excitation behavior of the gear mesh is analyzed by the detected rotational acceleration using angular rotation measurement systems. Subsequently, the transfer path between the gear meshes is determined to evaluate the mutual interactions between source and receiver. Based on the results, a guideline will be provided which stage has to be focused during the design phase.

Keywords Gearbox · Gears · Dynamic · Acoustic · Noise · Two-stage

1 Introduction

Multi-stage cylindrical gearboxes are widely used in drive technology, e.g. machine tools, automotive industry or wind turbines. Besides a sufficient load capacity and a maximum efficiency of a gearbox [1], the acoustic behavior gains in importance because of the increasing customer requirements or amended law restrictions. Decent development trends like the electrification of the drive train demand for the improvement of the gearbox noise behavior because of the lack of masking components, e.g. combustion engine [14]. According to Cerrato and Goodes, the noise generation process of multi-stage gearboxes can be divided into source, path and receiver [7]. The source is the excitation within the gear mesh of the gear stages. This excitation is transferred as structure-borne and airborne noise by the transfer path to the receiver. In literature, the analysis of acoustic behavior is mainly focused on single-stage cylindrical gearboxes [11, 12] or other gear types, e.g. beveloids [2]. The influence of manufacturing tolerances on the noise behavior is investigated as well [6]. Because of the mutual interactions between the gear meshes at a multi-stage gearbox, the knowledge at single-stage gearboxes cannot be transferred without restrictions. Instead, basic computational and experimental investigations must be carried out on multi-stage gearboxes. Few scientific papers analyze the acoustic behavior of multi-stage gearboxes, but do not focus on the mutual interactions and different steps of excitation along the noise generation process.

Kubur et al. use a model with six degrees of freedom for theoretical analysis of multi-stage gearboxes, which can contain any number of gears. The model is validated through experimental results of a single-stage gearbox. Subsequently, several parameters are varied on the basis of a two-stage gearbox. The effect of the change of the intermediate shaft

✉ Marius Schroers
m.schroers@wzl.rwth-aachen.de

¹ Laboratory for Machine Tools and Production Engineering (WZL) of RWTH Aachen University, Steinbachstr. 19, 52074 Aachen, Germany

length, the bearing stiffness, the phase shift, and the orientation of the helix angle on the tooth and bearing force is evaluated [10]. Zhou et al. conduct acoustical research on two-stage gearboxes theoretically and experimentally. The comparison between measurement and simulation shows good correlation. Additional to the gear mesh frequency, there are also modulation frequencies which indicate an interaction between the gear meshes. The analysis of the appearing orders identifies the gear mesh which is responsible for the modulation [16]. Further results can be found in [3, 8, 15].

For this reason, a research project funded by the DFG (BR 2905/66-1) was initiated with the objective to develop a method for the noise optimization of multi-stage gearboxes regarding dynamic interactions and psychoacoustic metrics. Previous work focuses calculational analysis of the excitation and noise behavior based on existing gears from the preceding project BR 2905/32 [4, 5].

2 Objective and experimental test setup

The objective of the present paper is to investigate the excitation and noise behavior experimentally with existing gear sets on the basis of a two-stage prototype gearbox. For this purpose, a drive train is designed for the experimental investigation of two-stage gearboxes and is equipped with measurement technology. Based on this, the dynamic excitation behavior of the gear sets is investigated. Finally, based on the noise generation process, transfer path analysis and the analysis of the airborne noise are performed. In order to investigate the noise behavior, two macro-geometric variants are selected. Both variants have an identical normal pressure angle, helical angle, gear ratio and face width. The first variant (gear set I (GSI)) described below as a reference has a normal module of $m_n = 3.5$ mm and a number of teeth of pinion and gear of $z_1/z_2 = 25/36$. The outer diameters are $d_a = 101.0/140.0$ mm. On the other hand, the second variant (GSII) has a normal module of $m_n = 3.0$ mm and the number of teeth are $z_1/z_2 = 29/42$. The outer diameters are $d_a = 98.6/138.2$ mm. The test gearbox is equipped with two macro-geometrically identical gear sets and therefore has a total gear ratio of 2.074 (GSI) and 2.098 (GSII). In order to investigate the shaft stiffness of the connecting shaft between the gear stages, a second shaft geometry is analyzed in addition to the reference variant. For the design of the second shaft geometry, the diameters between the two gears of the connecting shaft were reduced to half. At the same time, sufficient strength during operational usage as well as the possibility of integrating a supporting floating bearing into the test set-up has been taken into consideration.

For the tests, a two-stage prototype gearbox has been developed. The design characteristics of the gearbox are

described in the works of Brecher et al. in detail [4]. The test gearbox is integrated into the drive train set-up on the WZL's universal gearbox test rig. The universal gearbox test rig has an acoustic noise cabin, which according to DIN EN ISO 3744 represents a low-reflection half-space [13]. The input and output machines are located outside the noise cabin and are mounted on their own aerostatic mounted tensioning panels, just like the cabin. The machines can be connected to the drive train through cable ducts in the wall of the noise cabin. The power transmission between the machine and the test gearbox is transmitted on the drive side via constant-velocity joint shafts and a coupling made of natural rubber in order to decouple the excitation characteristics of the driving machine. On the output side, the connection is realized via a constant-velocity joint shaft and a cardan shaft. In order to keep the proportion of the external noise in the air-borne noise signal as low as possible, the components, which are necessary for the power transmission, are encapsulated in soundproof boxes during the acoustic test runs.

The test gearbox is shown in the middle upper part of Fig. 1. The measurement equipment applied in the test setup can be divided into three categories with reference to Fig. 1 along the source-path-receiver principle. The differential acceleration is selected as the measured variable for identifying the excitation source in the gear mesh. As the work of Brecher et al. and Carl shows, the measurement of the gear mesh excitation in the immediate vicinity of the gears is recommended [3, 6]. The information loss along the vibration transfer path between gear mesh and measuring system is thereby minimized.

Therefore, a rotational acceleration measuring system is applied directly next to each gear [4]. Using the base radii r_{bi} , the rotational accelerations $\ddot{\varphi}_i$ can be converted to the translational differential acceleration $\Delta\ddot{x}_i$ in the direction of the line of action using the equations in Fig. 1 on the left.

The transfer path is examined by means of structure-borne noise sensors, which are applied to the housing surface. Nine measuring points are selected in the vicinity of the bearings. A single-axis acceleration sensor is applied to each of the four externally accessible bearings in the x- and y-direction. The remaining sensor is mounted in the x-direction in the middle axis between the input and output.

Five free-field microphones are used to measure the air-borne noise. The arrangement of the microphones is shown in Fig. 1 on the right.

3 Dynamic excitation behavior of the gear meshes

3.1 Reference gear set

In this section, the gear set excitation properties are tested under dynamic operating conditions. The focus here lies

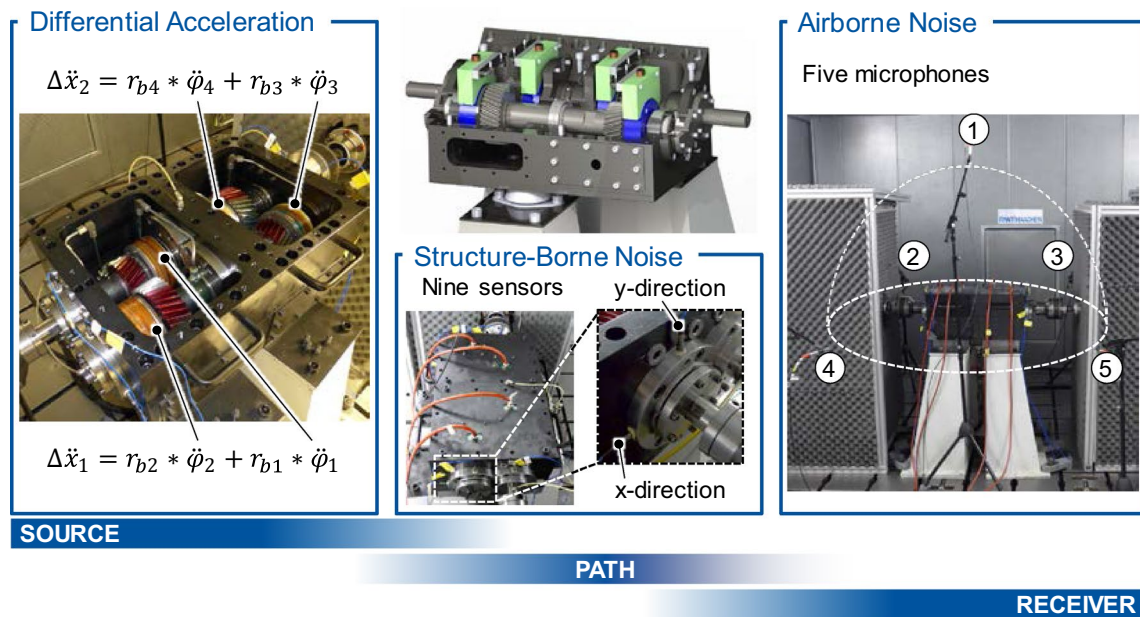


Fig. 1 Test gearbox with measurement equipment

on the dynamic interactions between the gear stages. In reference to the work of Brecher et al., a gear set with a low excitation level, which has been designed for acoustical investigations, is initially selected on both gear stages [4, 9]. This gear set is referred to as gear set I (GSI). The dynamic investigations are carried out for ideal rotational speed run-ups of $n_{in} = 300\text{--}3000$ rpm and a speed change rate of $\Delta n_{in}/\Delta t = 26.67$ rpm s^{-1} at a constant driving torque of $M_{in} = 325$ N m. In this case, the driving machine is operated in a torque-controlled manner and the driven machine is operated in a speed-controlled manner.

The results of the rotational speed run-ups of both gear stages are shown in Fig. 2. The diagrams show the frequency spectra averaged over the rotational speed and the order spectra of the differential acceleration referred to the rotational speed of input shaft 1. The representation as an averaged frequency spectrum in the upper row allows for the identification of speed-independent natural frequencies of the test setup. These occur through peaks in the spectrum.

The frequency spectrum of the first stage can be divided into three areas. In the low frequency range between $f = 100$ Hz and $f = 500$ Hz, natural frequencies with a low excitation level occur. The second range, which is dominated by the first gear mesh orders of the two stages, is between $f = 800$ Hz and $f = 1250$ Hz. The dominating peak is at $f = 1250$ Hz, at which the first gear mesh order reaches the end of the run-up. The third region is composed of a group of several natural frequencies between $f = 2000$ Hz and $f = 5000$ Hz, which is excited by the harmonic gear mesh orders. The frequency spectrum of the second stage can also be divided into the three frequency ranges. However, the

natural frequencies between $f = 1250$ Hz and $f = 5000$ Hz are more strongly excited, so that a higher excitation level is present in this frequency range.

The averaged order spectra in the lower part of Fig. 2 are evaluated referring to the rotational speed of shaft 1. The order of the first stage corresponds to the 25th order (orange arrows). On the other hand, the order of the second stage with respect to shaft 1 is the 17.4th order (red arrows). Both orders and their higher harmonic orders can be seen in the order spectra of both gear stages. In the order spectrum of the first stage, the orders of the first stage, the 25th order and their harmonics, have the highest excitation levels. In addition to the level-dominating first gear mesh order, the second and third gear mesh orders of the first stage have a high excitation level as well. On the other hand, the orders of the second stage, 17.4th order, and their harmonics prevail the order spectrum of the second stage. This is mainly due to the increasing excitation level from the first to the third gear mesh order. The effect of the higher excitation of the harmonic orders leads to a higher excitation in the acoustically relevant frequency range between $f = 1$ kHz and $f = 5$ kHz. An increased excitation can be seen in this frequency range in the averaged frequency spectrum.

From these considerations, the following central statements can be derived: On the one hand, the test setup has several eigenmodes between $f = 1$ kHz and $f = 5$ kHz in the acoustically relevant frequency range, which are excited by the gear mesh frequencies of both gear stages and their interactions. On the other hand, the higher harmonic excitation orders are responsible for the increased excitation in this frequency range. The first gear mesh order contributes,

- **Operating conditions**
 - M_{in} = 325 Nm
 - n_{in} = 300 – 3000 rpm
 - $\Delta n_{in}/\Delta t$ = 26.67 rpm s⁻¹
- **Gear set**
 - a = 112.5 mm
 - α_n = 20°
 - β = -19.3°/19.3°
 - m_n = 3.5 mm
 - z_1/z_2 = 25/36
- **Analysis parameter**
 - Differential acceleration
 - Order reg. shaft 1:
 - Stage 1: 25th order ←
 - Stage 2: 17.4th order ←

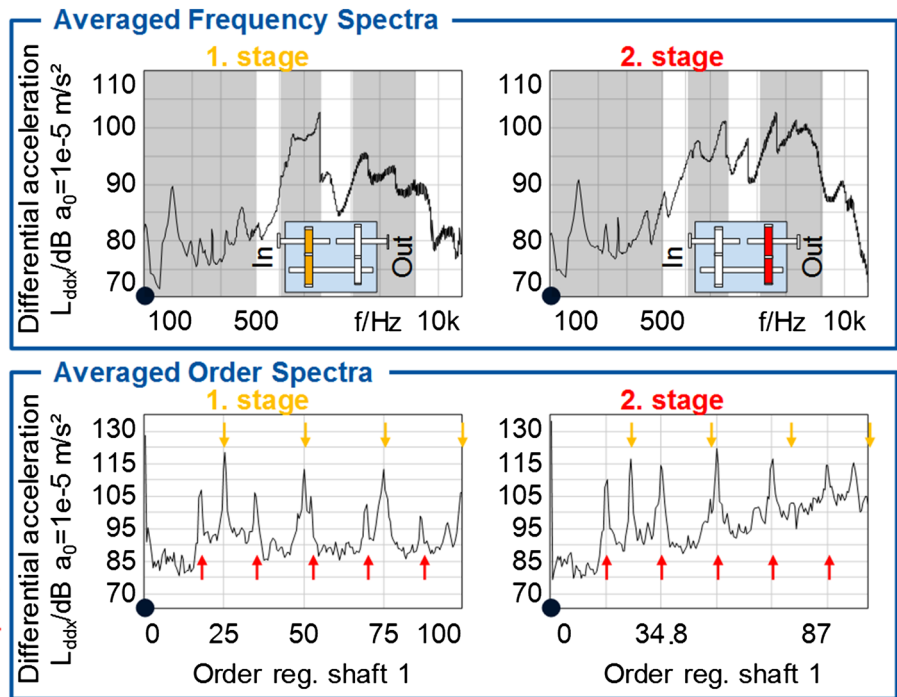


Fig. 2 Excitation behavior of the reference gear set (GSI)

solely or co-determinatively, to the dominant excitation level peak over the entire frequency range. When analyzing the interactions between the gear stages, it can be stated that the output stage is more influenced by the excitation orders of the first input stage than in the reverse case. Thus, the fast-rotating first stage has a higher acoustic relevance to the overall excitation spectrum. An optimization of this stage therefore offers a good potential for improving the excitation behavior of the gearbox. Therefore, the focus for improvements in the design phase should always lie on the fast-rotating first stage when optimizing the excitation behavior of a multi-stage gearbox.

3.2 Influence of the number of teeth

The number of teeth of both gear stages determines the frequency composition of the excitation spectrum and the noise spectrum. For this reason, in addition to the considered reference gear set (GSI), a second macro-geometric gear set (GSII) is tested with the same ratio. The results of the dynamic differential acceleration at equal operating conditions as for GSI are shown in Fig. 3. The already determined three frequency ranges can be identified in the averaged frequency spectrum of the two gear stages as well. In the first region below $f = 500$ Hz, both gear stages have comparable excitation levels. In both frequency spectra, the frequency range between $f = 800$ Hz and $f = 1450$ Hz is dominant. On the other hand, the

frequency range with a high number of eigenmodes between $f = 2000$ Hz and $f = 5000$ Hz in the spectrum of the first stage has an higher excitation level. In this frequency range, the higher-harmonic gear mesh orders contribute decisively to the excitation level.

Therefore, for the gear set II with a higher number of teeth, the averaged order spectrum is analyzed in the lower part of Fig. 3. The orders of the first gear stage correspond to the 29th order (orange arrows) and the orders of the second stage to the 20th order (red arrows). The order spectrum of the first stage is dominated by the gear mesh orders of the first stage (25th order and their harmonics). It is striking that the third gear mesh order has the highest excitation level. The third gear mesh order of the first stage therefore contributes decisively to the increased excitation level in the frequency spectrum up to $f = 4400$ Hz. In the averaged order spectrum of the second stage, increased excitation levels of the second stage occur (20th order and their harmonics). The highest excitation levels are the third and fourth gear mesh order of the second stage as well as the first gear mesh order of the first stage.

Thus, the conclusions reached for the reference variant (GSI) can be confirmed for the gear set II. For this gear set, the harmonic gear mesh orders must also be regarded due to the high excitation levels. The higher acoustic significance of the fast-rotating input stage can also be ascertained for this gear set, since the first gear mesh orders are transferred heavily (from the first to the second stage)

- **Operating conditions**
 - M_{in} = 325 Nm
 - n_{in} = 300 – 3000 rpm
 - $\Delta n_{in}/\Delta t$ = 26.67 rpm s⁻¹
- **Gear set**
 - a = 112.5 mm
 - α_n = 20°
 - β = -19.3°/19.3°
 - m_n = 3.0 mm
 - z_1/z_2 = 29/42
- **Analysis parameter**
 - Differential acceleration
 - Order reg. shaft 1:
 - Stage 1: 29th order ←
 - Stage 2: 20th order ←

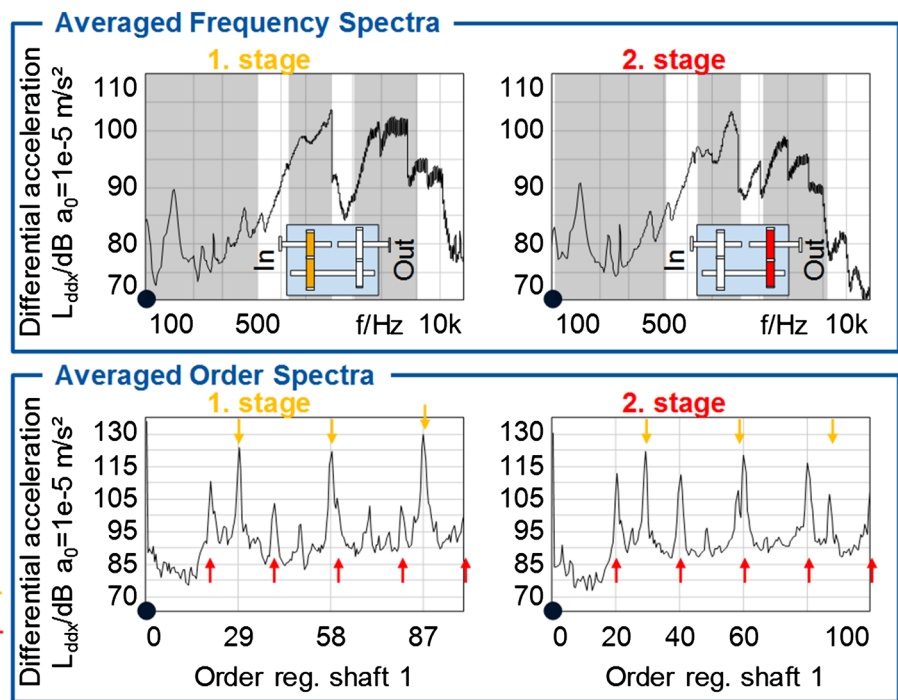


Fig. 3 Excitation behavior of the gear set II (GSII)

or less strongly (from the second to the first stage) between the gear stages.

3.3 Influence of the shaft geometry

To evaluate the influence of the shaft stiffness of the connecting shaft on the excitation behavior, the reference gear set (GSI) is selected and investigated using a alternated shaft geometry. For this geometry, the diameter of the intermediate shaft between the gears is reduced to half ($d_{Sha-Ref} = 60$ mm, $d_{Sha-Red} = 30$ mm). For comparative analysis, the profiles of the reference shaft from Fig. 2 are inserted in Fig. 4. In black, the courses of the reference shaft are opposed to the blue courses with a reduced shaft diameter. In the averaged frequency spectra in the upper part of the picture, a low natural frequency, which is shifted downwards at $f = 320$ Hz, has a higher excitation level at both gear stages. This can be explained by the reduced shaft stiffness. In addition, the frequency range up to $f = 1250$ Hz is dominated by the increased excitation level of the first gear mesh order.

This observation can be confirmed by the analysis of the averaged order spectrum in the lower part of Fig. 4. The gear mesh orders of the first stage have an increased excitation level in the order spectrum of the first stage. On the other hand, the orders excited by the second gear stage are less strongly transmitted by the reduced shaft stiffness, so that lower levels occur here. The order spectrum of the second stage shows analogous effects. Only the excitation level of

the first gear mesh order of the second stage has an increased excitation level. The excitation orders of the first stage, on the other hand, are transmitted less to the second stage.

Thus, it can be determined that the changed shaft geometry significantly influences the excitation behavior. On the one hand, the dynamic excitation behavior of the gearbox is more strongly excited by the reduced shaft geometry. On the other hand, the interactions between the gear stages are reduced by the lower stiffness of the connection shaft. The design of the connecting shaft between the gear stages consequently involves the compromise between a low system excitation and low interactions between the gear stages. The mutual influence will be investigated in more detail in the following chapter.

4 Machine acoustic transfer behavior

4.1 Analysis of the mutual influence between the gear stages

In order to analyze the interactions between the gear stages, the order cuts of the 25th order for the two shaft geometries are shown in Fig. 5. In each case, the excitation of the first gear mesh order of the first stage is compared with the transferred excitation of the same order at the second stage. For both shaft geometries, the excitation level at the first stage is in a wide frequency range above the excitation level at

Operating conditions

- $M_{in} = 325 \text{ Nm}$
- $n_{in} = 300 - 3000 \text{ rpm}$
- $\Delta n_{in}/\Delta t = 26.67 \text{ rpm s}^{-1}$



Gear set

- $a = 112.5 \text{ mm}$
- $\alpha_n = 20^\circ$
- $\beta = -19.3^\circ/19.3^\circ$
- $m_n = 3.5 \text{ mm}$
- $z_1/z_2 = 25/36$

Analysis parameter

- Differential acceleration

Legend

- Reference shaft 
- Reduced shaft 

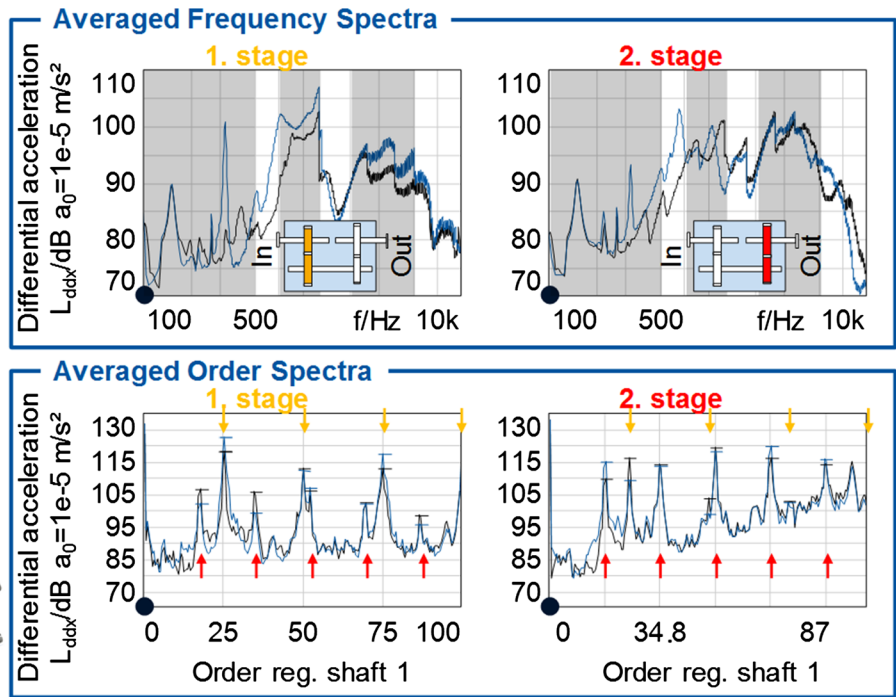


Fig. 4 Excitation behavior of the modified shaft geometry

Operating conditions

- $M_{in} = 325 \text{ Nm}$
- $n_{in} = 300 - 3000 \text{ rpm}$
- $\Delta n_{in}/\Delta t = 26.67 \text{ rpm s}^{-1}$

Gear set

- $a = 112.5 \text{ mm}$
- $\alpha_n = 20^\circ$
- $\beta = -19.3^\circ/19.3^\circ$
- $m_n = 3.5 \text{ mm}$
- $z_1/z_2 = 25/36$

$G(j\omega) = \frac{\Delta \ddot{x}_{25.Ord-2st}(j\omega)}{\Delta \ddot{x}_{25.Ord-1st}(j\omega)}$

Legend

- Measurement at stage 1
- Measurement at stage 2
- Transfer function

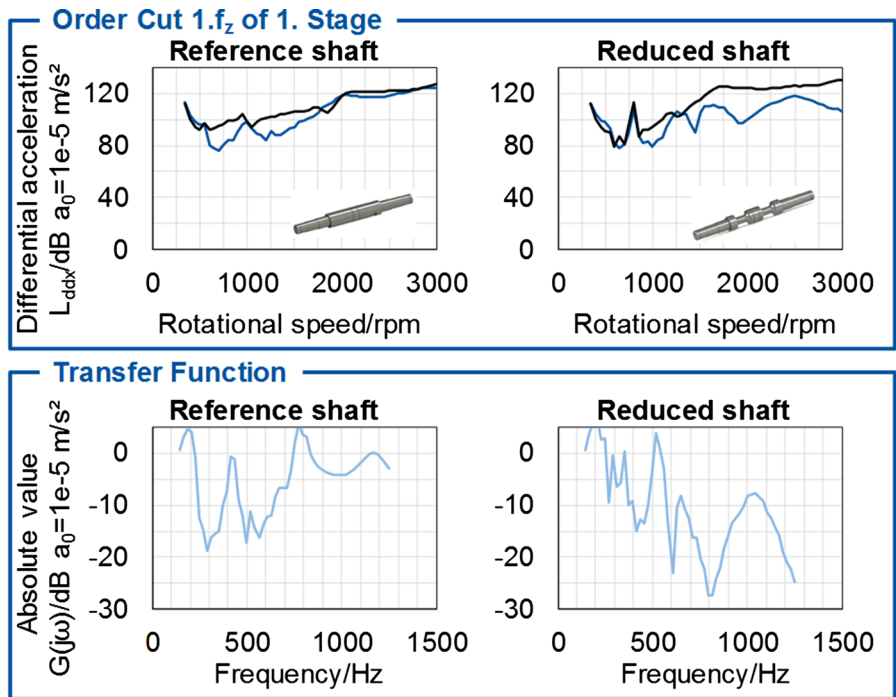


Fig. 5 Transfer function of the modified shaft geometry

the second stage. In the case of the reduced shaft geometry, the reduced vibration transfer is noticeable initiating from a speed of $n = 1400 \text{ rpm}$.

For further analysis of the phenomenon, the transfer function between the two courses shown in the upper half is shown in the lower half of Fig. 5. The transfer function

of the 25th order $G(j\omega)$ is calculated according to Eq. (1). The excitation at the first stage $\Delta\ddot{x}_{25.Ord-1st}(j\omega)$ is used as the input variable and the excitation at the second stage $\Delta\ddot{x}_{25.Ord-2st}(j\omega)$ as the output variable.

$$G(j\omega) = \frac{\Delta\ddot{x}_{25.Ord-2st}(j\omega)}{\Delta\ddot{x}_{25.Ord-1st}(j\omega)} \tag{1}$$

The absolute value of the transfer function shows areas of strong and weak vibration transfer for both shaft geometries. In the frequency range up to $f = 700$ Hz, strong transfer points coincide with the natural frequencies of the system. For the reduced shaft geometry, the transfer behavior decreases from a frequency between $f = 700$ Hz and $f = 1250$ Hz. As a result, there is little mutual influence in this area. However, with a natural frequency of the system in the range of $f = 1100$ Hz, the vibration transfer increases in this range.

The choice of the shaft geometry thus reduces the mutual influence. For distinct frequency ranges, the vibration transfer between the gear stages can be reduced. For gearboxes with a constant working point, the design of the connecting shaft can lead to a lower interaction between the gear stages. Thus, the shaft design reduces the interaction in the frequency range of the working point. In the design, however, the changing dynamic behavior of the system and the shifting of natural frequencies must be

taken into account so that there is no increased overall excitation level.

4.2 Analysis of the transfer path between source and receiver

The airborne noise signal from the microphone 1, which is positioned centrally above the gearbox see Fig. 1, is shown in blue in Fig. 6 for the gear set II. In the areas between the gear mesh orders, there is a higher excitation level which does not result from the excitation in the gear mesh and thus can be identified as extraneous noise components. However, the gear mesh orders are still to be identified as distinctly superior excitation orders. The courses of the other four microphones, numbers 2–5 cf. Fig. 1, show similar characteristics. Thus, only the airborne noise signal of microphone 1 is shown in this paper.

The comparison between the received airborne noise and the gear mesh excitation, differential acceleration marked in black, is shown in Fig. 6 for the two stages. The gradation of the excitation and noise levels of the 58th and the 60th order match for the first stage in the upper row. The 58th order has the higher level and the 60th order the lower level. For the second stage in the lower row, the levels gradation between the two orders change between the differential acceleration to the airborne noise. For the differential acceleration, the 58th order has a lower excitation level than the 60th order. In contrast, the levels are reversed for the noise pressure.

- Operating conditions
 - $M_{in} = 325$ Nm
 - $n_{in} = 300 - 3000$ rpm
 - $\Delta n_{in}/\Delta t = 26.67$ rpm s^{-1}
- Gear set
 - $a = 112.5$ mm
 - $\alpha_n = 20^\circ$
 - $\beta = -19.3^\circ/19.3^\circ$
 - $m_n = 3.0$ mm
 - $z_1/z_2 = 29/42$
- Analysis parameter
 - Differential acceleration
 - Airborne noise at micro 1
- Legend
 - Differential acceleration
 - Airborne noise

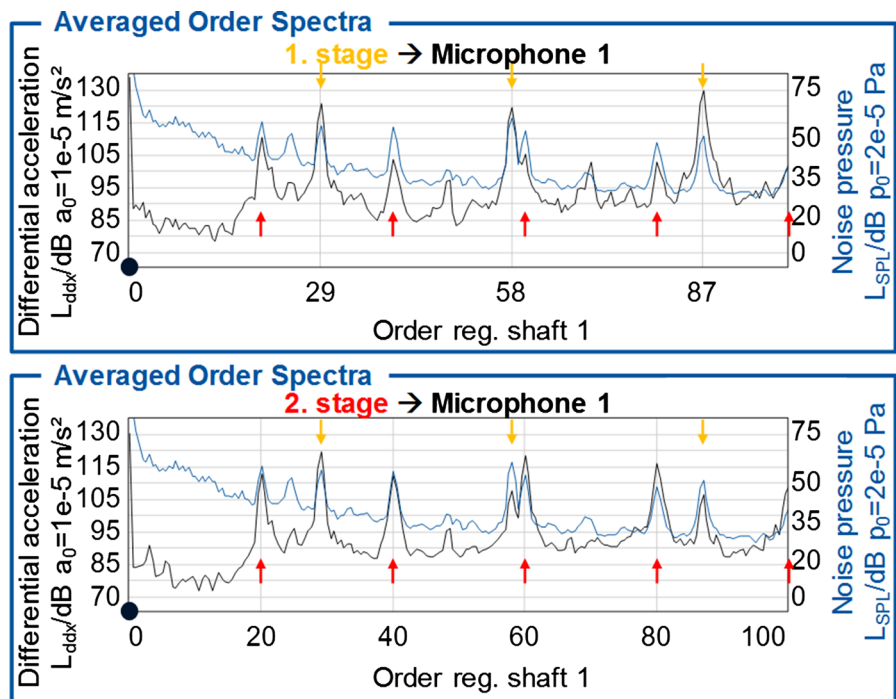


Fig. 6 Correlation between gear mesh excitation and airborne noise (GSII)

Subsequently, it can be stated that the first stage predominant defines the excitation levels of the airborne noise spectrum. Thus, the optimization of the design of the first stage has a high potential regarding the improvement of the noise behavior of multi-stage gearboxes.

5 Summary and outlook

Multi-stage cylindrical gearboxes are often used in drive trains, in which the excitation and noise behavior becomes more and more important as a quality criterion. The running behavior can be divided into the analysis of the excitation behavior and the analysis of the noise behavior of the emitted noise.

According to the machine acoustic noise generation, measurement equipment is applied to the two-stage gearbox. The gear mesh excitation is measured with rotational acceleration sensors. The structure-borne noise is analyzed by means of acceleration sensors and microphones are applied to measure the emitted airborne noise. The parameters investigated in this report are the stiffness of the connecting shaft between the gear stages and a variation of the number of teeth of the gear sets.

For both gear sets, the analysis of the gear mesh excitation shows the characteristic gear mesh orders. Furthermore, the excitation behavior is dominated by the first stage, which has the higher rotational speed. Thus, the reduction of the excitation level of the first stage provides high potential for a reduction of the whole excitation level of the gearbox. Therefore, the first stage should be focused in the design phase. Due to the transfer function of the modified shaft geometry, a reduced transfer of structure-borne noise between the gear meshes is observed. For distinct frequency ranges, the interaction between the gear stages can be reduced or eliminated. In addition, a higher excitation level for the modified shaft is caused by a displaced natural frequency. The frequency range, in which the vibration transfer is reduced, depends on the shaft geometry and has to be taken into account in the design phase. Furthermore, the comparison between the excitation of the gear meshes and the airborne noise confirms that the first stage dominates the noise behavior.

As a next step, the simulation model of [4] has to be validated with the experimental results of this report. Based on the validated simulation model, a detailed parametric study can be carried out, which is evaluated by means of a sensitivity analysis. The sensitivity analysis includes the investigation of the influence of manufacturing tolerances and of interactions between the deviations of the gear stages on the noise behavior. The final step is the psychoacoustic evaluation of both, computational and experimental results.

Acknowledgements The authors would like to thank the German Research Foundation (DFG) for funding the research project “Entwicklung einer Methode zur Geräuschoptimierung zweistufiger Getriebe unter Berücksichtigung dynamischer Zusammenhänge” (BR 2905/66-1).

References

1. Babichev D, Storchak M (2015) Synthesis of cylindrical gears with optimum rolling fatigue strength. *Prod Eng Res Devel* 9(1):87–97. <https://doi.org/10.1007/s11740-014-0583-6>
2. Brecher C, Brumm M, Hübner F, Henser J (2013) Influence of the manufacturing method on the running behavior of beveloid gears. *Prod Eng Res Devel* 7(2–3):265–274. <https://doi.org/10.1007/s11740-012-0442-2>
3. Brecher C, Gorgels C, Hesse J, Hellmann M (2011) Dynamic transmission error measurements of a drive train. *Prod Eng Res Devel* 5(3):321–327. <https://doi.org/10.1007/s11740-011-0310-5>
4. Brecher C, Löpenhaus C, Schroers M (2016) Analysis of excitation behavior of a two-stage gearbox based on a validated simulation model. In: AGMA (Hrsg) Fall technical meeting
5. Brecher C, Löpenhaus C, Schroers M (2017) Analysis of dynamic excitation behavior of a two-stage spur gearbox. *Procedia CIRP* 62:369–374. <https://doi.org/10.1016/j.procir.2016.06.027>
6. Carl C (2014) Gehörbezogene Analyse und Synthese der vibroakustischen Geräuschanregung von Verzahnungen. Diss., RWTH Aachen University
7. Cerrato G, Goodes P (2011) Practical approaches to solving noise and vibration problems. *So Vib Mag* 45(4):18–22
8. Cheon G-J (2010) Numerical study on reducing the vibration of spur gear pairs with phasing. *J Sound Vib* 329(19):3915–3927
9. Hohle A (2002) Auswirkungen von Rauheit Oberflächenstruktur und Fertigungsabweichung auf das Lauf- und Geräuschverhalten hartfeinbearbeiteter hochüberdeckender Zylinderräder. Diss., RWTH Aachen University
10. Kubur M, Kahraman A, Zini DM, Kienzle K (2004) Dynamic analysis of a multi-shaft helical gear transmission by finite elements. *Model Exp J Vib Acoust* 126(3):398–406. <https://doi.org/10.1115/1.1760561>
11. Möllers W (1982) Parametererregte Schwingungen in einstufigen Zylinderradgetrieben. Einfluß von Verzahnungsabweichungen und Verzahnungssteifigkeitsspektren. Diss., RWTH Aachen University
12. Müller R (1991) Schwingungs- und Geräuschanregung bei Stirnradgetrieben. Diss., TU München
13. Norm (2011) Akustik Bestimmung der Schalleistungs- und Schallenergiepegel von Geräuschquellen aus Schalldruckmessungen. Hüllflächenverfahren der Genauigkeitsklasse 2 für ein im Wesentlichen freies Schallfeld über einer reflektierenden Ebene 14.140.01(3744). Beuth, Berlin
14. Steinberg KF (2007) With all senses. The first book on how to eliminate interfering sound in the car, 1. Aufl. wjr-reference book. wjr-Verl., Eching
15. Vinayak H, Singh R, Padmanabhan C (1995) Linear dynamic analysis of multi-mesh transmissions containing external, rigid gears. *J Sound Vib* 185(1):1–32
16. Zhou C, Young S, Tang Y (2011) Two-stage gear driveline vibration and noise. SAE Int, Pennsylvania